Transportation Research Part C 92 (2018) 472–485

Contents lists available at ScienceDirect

Transportation Research Part C

journal homepage: www.elsevier.com/locate/trc

Dynamic operations and pricing of electric unmanned aerial vehicle systems and power networks

Kaiqing Zhang[a], Liqun Lu[b], Chao Lei[b], Hao Zhu[c], Yanfeng Ouyang[b,*]

[a] Department of Electrical and Computer Engineering, University of Illinois at Urbana-Champaign, Urbana, IL 61801, USA
[b] Department of Civil and Environmental Engineering, University of Illinois at Urbana-Champaign, Urbana, IL 61801, USA
[c] Department of Electrical and Computer Engineering, The University of Texas at Austin, Austin, TX 78705, USA

ARTICLE INFO

Keywords:
Unmanned aerial vehicle
Electricity pricing
Demand response
Aviation transportation

ABSTRACT

The emergence of electric unmanned aerial vehicle (E-UAV) technologies, albeit somewhat futuristic, is anticipated to pose similar challenges to the system operation as those of electric vehicles (EVs). Notably, the charging of EVs en-route at charging stations has been recognized as a significant type of flexible load for power systems, which often imposes non-negligible impacts on the power system operator's decisions on electricity prices. Meanwhile, the charging cost based on charging time and price is part of the trip cost for the users, which can affect the spatio-temporal assignment of E-UAV traffic to charging stations. This paper aims at investigating joint operations of coupled power and electric aviation transportation systems that are associated with en-route charging of E-UAVs in a centrally controlled and yet dynamic setting, i.e., with time-varying travel demand and power system base load. Dynamic E-UAV charging assignment is used as a tool to smooth the power system load. A joint pricing scheme is proposed and a cost minimization problem is formulated to achieve system optimality for such coupled systems. Numerical experiments are performed to test the proposed pricing scheme and demonstrate the benefits of the framework for joint operations.

1. Introduction

Electric unmanned aerial vehicles (E-UAVs), also called electric drones, are usually referred to as battery-powered, autonomous aircrafts propelled by multiple rotors. In recent years, rapid advances in control technologies and diminishing costs have led to increasing utilization of UAVs, especially E-UAVs, for various civilian purposes, such as aerial surveillance/mapping (Maini and Sujit, 2015; Nintanavongsa et al., 2016; Pugliese et al., 2016; Kaufmann et al., 2018), entertainment (Guerriero et al., 2014), as well as transportation of goods in times of critical need (Kim et al., 2017; Stewart, 2014; Thiels et al., 2015; Ham, 2018). In particular, the booming growth of e-commerce and customers' increasing needs for fast delivery have motivated many leading logistics companies to explore the use of E-UAVs for parcel delivery. For example, Amazon announced its Prime Air in 2013, which is an E-UAV delivery system designed to deliver packages up to five pounds to customers in 30 min or less (Mattise, 2013). German firm DHL launched its Parcelcopter research project in December 2013 (Hern, 2014). More recently, UPS has also unveiled its drone delivery plan, in which E-UAVs can be launched from trucks at selected points along the truck routes (Vanian, 2017).

The aviation industry's interest in E-UAVs has gone beyond aerial surveillance and freight delivery, and has turned toward passenger transportation. Recently, Zunum Aero, a company funded by Boeing and JetBlue, revealed its plan to create a hybrid

* Corresponding author.
E-mail address: yfouyang@illinois.edu (Y. Ouyang).

https://doi.org/10.1016/j.trc.2018.05.011
Received 8 September 2017; Received in revised form 9 May 2018; Accepted 10 May 2018
Available online 28 May 2018
0968-090X/

electric aircraft that can offer cheap commuter flights by 2020 (Etherington, 2017). The U.S. flying-car startup, Terrafugia, is aiming to have its autonomous flying vehicle, called the TF-X, flying commercially by 2025 (Muoio, 2016). The German startup Volocopter, which launched in 2011 the first helicopter powered solely by electricity, is also developing the fleet of air taxis (Muoio, 2017). Another German startup called Lilium Aviation successfully completed a test flight of its all-electric, vertical take-off and landing (VTOL), two-seater prototype in April 2017 (Hawkins, 2017). As such, while E-UAVs have not been put into commercial use quite yet, we believe that it is only a matter of time for wide applications of E-UAVs to appear in the very near future.

Many challenges that have arisen nowadays for traditional electric vehicles (EVs) can be anticipated for future applications of E-UAVs, mainly due to their similarities in terms of energy source and recharging needs. In particular, even with recent battery recharging technologies, EVs still have relatively limited travel ranges and long charging times. Such limitations have led to numerous studies on planning infrastructure and traffic routing for en-route EVs (Chen et al., 2016; Worley and Klabjan, 2011; Worley et al., 2012). Similarly, even though many efforts have been put into developing E-UAV technologies, the short flight range owing to limited battery capacity still poses a great challenge. Several strategies have been proposed to overcome the range limitations of E-UAVs. Some researchers have put their focuses on designing a multi-modal truck-drone delivery system, where drones are carried to the vicinity of customers by a fleet of trucks so as to cover only "the last mile" (Agatz et al., 2018; Ferrandez et al., 2016; Ha et al., 2015; Luo et al., 2017; Murray and Chu, 2015; Poikonen et al., 2017; Wang et al., 2017), where E-UAVs are launched at stops along the truck routes and return to the trucks after delivery. Alternatively, Sundar and Rathinam (2012, 2014) introduced a so-called fuel-constrained E-UAV routing problem, where an E-UAV is allowed to refuel/recharge at any of refueling depots such that all delivery targets are visited and the total fuel consumption is minimized. Along this direction of inquiry, some researchers examined E-UAV systems supported by automated refueling stations that enable long-term or persistent services (Kim et al., 2013; Kim and Morrison, 2014; Song et al., 2014, 2016; Hong et al., 2018). Dorling et al. (2017) proposed a multi-trip vehicle routing model that allows multi-rotor E-UAVs to make multiple returns to the depot to replace batteries. Most of these studies assumed that the batteries can be replaced instantly or the charging time is negligible. Therefore, no consideration is cast over the impacts of charging activities on not only the E-UAV operations, but also the associated infrastructures (such as charging stations and the underlying power grids).

However, we can foresee that the huge electricity demand from E-UAV charging, in particular for en-route charging from inter-city trips of E-UAVs, would pose a great impact on power grids, just similar to the challenges faced by the EV industry nowadays (Ma et al., 2012; Xu and Pan, 2012). Furthermore, since the travelers' en-route charging decisions are highly related to their travel behaviors (Sweda and Klabjan, 2012; He et al., 2014; Adler et al., 2016), it is imperative to investigate the interactions and joint operations of the coupled power and transportation systems. Some earlier efforts have been made towards the EV practice; e.g., Alizadeh et al. (2015) proposed a joint charging pricing mechanism that maximizes the welfare of both travelers and power generators, assuming travelers' travel choices can be controlled via proper roadway tolls. He et al. (2013) considered an equilibrium framework that captures the interactions among the availability of public charging opportunities, the charging prices, and the route choices of EVs. Even though these studies mainly focus on a static setting, they indeed remind us of potential challenges that might occur when E-UAVs become commercialized for both freight and passenger transportation.

In this paper, we consider the operations of a coupled system of aviation transportation and power networks, and address the temporal fluctuation of electricity prices caused by *time-varying* E-UAV travel demand and power base loads. Although it is known that both the power and aviation transportation systems may be ideally operated in a demand-responsive and dynamic way, there is still likely a long way ahead before we achieve that status, because of technical and regulatory barriers. As an initial step toward the foreseeable future, this study focuses on a possible scenario that may occur in the next 5–10 years. Hence, we assume that the anticipated systems still share some similarities with the current ones: (i) For the power system, we assume a day-ahead wholesale electricity market (which is the current industry practice (US Federal Energy Regulatory Commission, 2003)), where the locational marginal prices (LMPs) of electricity (Glover et al., 2011), power commitments and demand for the 24 h of the next day are determined beforehand. In such a day-ahead market, there is a non-profit independent system operator (ISO) responsible for determining the LMPs and maintaining a regulated platform where market participants can submit supply offers or demand bids a day before. The power generators receive the posted LMPs from the ISO, and decide their generation amount to maximize their own utilities; (ii) For the aviation transportation system, to assure safe and high-quality service for travelers, we assume that the system is centrally monitored and controlled just like the current practice of the aviation industry, where E-UAVs' tentative travel needs are submitted at least 24 h prior to the travels, and then the aviation agency assigns them with detailed routing and charging plans. Moreover, we assume that the E-UAVs of interest are owned by the individual travelers as personal vehicles (i.e., as a plausible business scenario in the near future), and we mainly focus on their applications for inter-city travels, where each trip requires a stop at one of the charging stations.[1] The short distance trips that do not need en-route charging are not included in this study, since the charging activities can be conducted at their origins and/or destinations (as part of the regular electricity loads there) and have little influence on either the charging stations (our focus of the study) or the travel plans. Moreover, due to the limited charging slots at charging stations, the agency would coordinate E-UAV users' travel plans as well as the charging timing, such that the usage of charging slots does not exceed the capacity.

We propose a joint pricing scheme for the electricity market that accounts for the costs of both systems, such that system-wide

[1] The proposed modeling approach can easily be extended to more general cases where a single trip involves multiple or no charging stops. For the multiple-stop case, this can be done by evaluating (possibly through full or partial enumeration) the E-UAV users' alternative routing decisions across charging stations (Adler et al., 2016), and adding the corresponding decision variables to the aviation agency's optimization problem. The non-stop trips are not considered in this study, since they have no impact on other E-UAVs' travel plans, and the charging at the origins or destinations (e.g., from users' residential power outlets) can be directly included as base load to the power system (Zhang et al., 2017a).

optimum can be achieved. An E-UAV assignment model is developed such that the cost for E-UAV users is minimized. The proposed model takes into account both the spatial and temporal variability of electricity prices and provides the flexibility of exploiting demand response via E-UAV charging. The main contributions of the present work are threefold: (i) we establish a joint optimization problem to minimize the total costs, accounting for the coupling between the dynamic E-UAV charging on the transportation system and the operation of power networks; (ii) we develop a dynamic E-UAV assignment problem with time-varying travel demand, flexible travel time, and limited charging slots at charging stations; (iii) we propose a joint pricing scheme that can induce both systems to achieve the system optimum collaboratively while preserving the private information from disclosure to each other.

This paper is organized as follows: in Section 2, a power generation model and a generic E-UAV assignment model are presented, and a system-wide cost minimization problem is formulated and an electricity pricing scheme is proposed to achieve the system optimum. Then Section 3 introduces a dual-decomposition-based approach to solve the minimization problem, followed by Section 4 where numerical examples are presented to demonstrate the effectiveness of the modeling framework. Finally, Section 5 provides a summary of this paper, highlights the insights revealed by the model, and proposes several future research directions.

2. Methodology

In this section, we illustrate how power and aviation transportation systems operate jointly in the electricity market. We first show how the power-side ISO determines and posts electricity prices to the generators and users in the electricity market. Then, we show how the aviation transportation agency would coordinate and determine travel plans for a group of users. At last, we investigate how the system optimum can be achieved for the coupled power and aviation transportation systems through a joint pricing scheme of the ISO.

2.1. Power generation model

The electricity market participants are connected via the power transmission network $\mathscr{R} = (\mathscr{B},\mathscr{F})$, where $\mathscr{B}$ and $\mathscr{F}$ are the sets of buses and extensive transmission lines, respectively. Each bus $i \in \mathscr{B}$ is a participant in the market that either generates or consumes power. For brevity, we assume that a single merged generator is located on each bus of the grid. Typically, the period of a day is discretized into a set of time slots $\Gamma = \{1,2,...,T\}$, indexed by τ. The LMPs and power consumption and generation within each time slot $\tau \in \Gamma$ are constant. For convenience, we let $\mathscr{T} := \{t_0,t_1,...,t_T\}$ be the set of time instants that separate one day into T disjoint periods $[t_0,t_1),[t_1,t_2),...,[t_{T-1},t_T)$, each with an equal length Δ (h), and we further assume that the planning horizon is periodic such that $t_\tau = t_{\tau \pm T}, \forall\, \tau \in \Gamma$. The generator at each bus $i \in \mathscr{B}$ aims at maximizing its profit, i.e., sales revenue minus power generation cost, given the LMPs in the market.[2] The power generation model for bus i can be formulated as follows:

$$\mathbf{GP}_i \qquad \min_{\mathbf{G}_i} \; C_i(\mathbf{G}_i) - \Delta \mathbf{p}_i^T \mathbf{G}_i \tag{1}$$

$$\text{s. t.} \quad |G_{i,\tau+1} - G_{i,\tau}| \leqslant R_i, \quad \forall\, \tau \in \Gamma, \tag{2}$$

$$\mathbf{G}_{i,min} \leqslant \mathbf{G}_i \leqslant \mathbf{G}_{i,max}, \tag{3}$$

where decision variables $\mathbf{G}_i \in \mathbb{R}^T$ is the vector of every $G_{i,\tau}$, the power generation at bus i at time slot τ (MW), and $\mathbf{p}_i \in \mathbb{R}^T$ is the vector of electricity LMP at bus i ($/MWh). Function $C_i(\cdot)$ captures the power generation cost at bus i, which is usually assumed to be strongly convex. In this study, we assume the generation cost function is quadratic (Glover et al., 2011), i.e.,

$$C_i(x) = a_{i,1}x^2 + a_{i,2}x, \tag{4}$$

where $a_{i,1}$ and $a_{i,2}$ are associated parameters. The inequalities (6) are referred to as ramp constraints, which prevent an extremely large increase or decrease in power generation at consecutive time slots. The ramp capacity $R_i > 0$ reflects the inherent thermal and mechanical inertia of generators at bus i, and this parameter should be admissible over the course of the optimization. Constraints (7) enforce upper and lower limits on the generated power. Note that we can aggregate problem $\mathbf{GP}_i, \forall\, i \in \mathscr{B}$ into one problem since the generators decisions are independent of each other; i.e.,

$$\mathbf{GP} \qquad \min_{\mathbf{G}_i, i \in \mathscr{B}} \; \sum_{i \in \mathscr{B}} C_i(\mathbf{G}_i) - \Delta \mathbf{p}_i^T \mathbf{G}_i \tag{5}$$

$$\text{s. t.} \quad |G_{i,\tau+1} - G_{i,\tau}| \leqslant R_i, \quad \forall\, \tau \in \Gamma, i \in \mathscr{B}, \tag{6}$$

$$\mathbf{G}_{i,min} \leqslant \mathbf{G}_i \leqslant \mathbf{G}_{i,max}, \quad \forall\, i \in \mathscr{B}. \tag{7}$$

In this way, the actual generated power per bus should be decided based on the LMPs posted to the generators.

[2] Here we assume generators are price-takers in the day-ahead wholesale market, which take the LMPs as input and determine the amount of generation in response. The case with strategic generators/price-anticipaters who influence market price (Hobbs et al., 2000; Xu et al., 2017) is left for future work.

2.2. E-UAV travel model

We consider the aviation transportation network as a complete graph of a set of nodes $\mathcal{O} \cup \mathcal{D} \cup \mathcal{S}$, where $\mathcal{O}$ and $\mathcal{D}$ are the sets of origins and destinations, respectively; $\mathcal{S} \subseteq \mathcal{B}$ is the set of charging stations which post the LMPs to E-UAV users and submit the demand bids to the ISO. Since the E-UAV transportation system is centrally controlled by an aviation agency, we assume that the E-UAV users need to submit: (i) their tentative travel plan, including origin $o \in \mathcal{O}$, destination $d \in \mathcal{D}$, preferred departure and arrival time t_{dep},$t_{arr} \in \mathcal{T}$; (ii) preferred battery charging level $y \in \mathcal{Y}$ (MWh) that the users wish to charge to when at a charging station,[3] and (iii) vehicle types $v \in \mathcal{V}$ capturing specifications such as maximum range and energy efficiency. Then the agency makes plans for all the users based on the information being supplied. For notational brevity, we use the sextuplet $q = (o,d,t_{dep},t_{arr},v,y)$ to denote the type of demand and let $\mathcal{Q}$ be the set of all travel demand types. The volume of travel demand of type q is denoted by u_q. Furthermore, charging power at charging stations are allowed to be location-specific, and we use β_s to denote the charging power at charging station $s \in \mathcal{S}$.

2.2.1. User's travel cost

For an E-UAV user of type q, the aviation agency needs to make plans for its actual departure time $t_\tau \in \mathcal{T}$ as well as its charging station $s \in \mathcal{S}$. The user's *travel cost*, denoted by c_q, contains three components: (i) transportation cost $c_{q,t}$; (ii) charging cost $c_{q,e}$; and (iii) unpunctuality penalty $c_{q,p}$ due to lateness/earliness of actual departure/arrival, i.e.,

$$c_q(t_\tau,s) = c_{q,t}(t_\tau,s) + c_{q,e}(t_\tau,s) + c_{q,p}(t_\tau,s)\ , \quad \forall\ q \in \mathcal{Q}. \tag{8}$$

Several additional assumptions need to be presented first to formulate the user's travel cost. We assume that the fleet size of E-UAVs is moderate such that aerial congestion is negligible. The travel route is thus composed of direct trip legs connecting the origin, the charging station, and the destination; it also implies that the transportation cost $c_{q,t}$ only depends on the choice of charging stations, i.e.,

$$c_{q,t}(t_\tau,s) = c_{q,t}(s) = \alpha_t \cdot (w_{o-s} + w_{s-d})\ , \quad \forall\ s \in \mathcal{S},\ q \in \mathcal{Q}, \tag{9}$$

where α_t is the monetary-millage conversion factor (\$/mile), and w_{o-s} and w_{s-d} are the distances (mile) from origin o to charging station s and from s to destination d, respectively.

In addition, we assume that E-UAVs always depart from origin with full battery capacity, and they charge the battery to their preferred level (or to the minimum levels that can exactly cover the rest of the trips). Different types of E-UAVs are associated with different full-battery ranges as well as charging efficiencies in terms of energy-range conversions, due to varying vehicle weights and motor technologies. Therefore, the charging time required for type-q E-UAV users to charge at station s can be computed as follows:

$$l_c(q,s) = \left\lceil \frac{1}{\beta_s} \max\left\{ \frac{w_{o-s} + w_{s-d} - w_v}{\alpha_v}, y - \frac{w_v - w_{o-s}}{\alpha_v}, 0 \right\} \right\rceil, \tag{10}$$

where α_v is the energy-range efficiency (mile/MWh), and w_v is the full-battery range of thetype-v vehicle. Eq. (10) means that the E-UAVs need to charge to at least the minimum level required to cover the rest of the trip, or to their preferred level, or that they do not need charging at all if their battery level is above their preferred charging level and the minimum required level when they arrive at the station. We use $\lceil \cdot \rceil$ to round the charging duration (and other time durations that will be introduced later) up to multiples of the time period length Δ to match our discrete time horizon.[4] Note that if $w_{o-s} > w_v$ or $w_{s-d} > w_v$, such a path is infeasible and should not be used; and if $(w_{o-s} + w_{s-d} - w_v) \leqslant 0$, such a trip does not require charging en route. Therefore, the charging cost is calculated based on the entire charging duration, i.e.,

$$c_{q,e}(t_\tau,s) = \sum_{\tilde{\tau}=\tau'}^{\tau'+l_c/\Delta} \beta_s \cdot \Delta \cdot p_{s,\tilde{\tau}}\ , \quad \forall\ t_\tau \in \mathcal{T},\ s \in \mathcal{S},\ q \in \mathcal{Q}, \tag{11}$$

where $t_{\tau'}$ is the time when the E-UAV arrives at the charging station and starts charging, i.e., $t_{\tau'}(t_\tau,s) = t_\tau + \left\lceil \frac{w_{o-s}}{v_a} \right\rceil$ with v_a being the travel speed of the E-UAV (mile/hr). Again, $p_{s,\tilde{\tau}}$ is the LMP of electricity at charging station s at time $t_{\tilde{\tau}} \in \mathcal{T}$ (\$/MWh). Clearly, the time at which the E-UAV completes charging and leaves for destination is $t_{\tau''}(t_\tau,s) = t_{\tau'}(t_\tau,s) + l_c$, and the earliest time of arrival at destination d is thus $t_{\tau'''}(t_\tau,s) = t_{\tau''}(t_\tau,s) + \left\lceil \frac{w_{s-d}}{v_a} \right\rceil$. The unpunctuality cost can thus be expressed as

$$c_{q,p}(t_\tau,s) = f_p(t_\tau - t_{dep}, t_{\tau'''} - t_{arr})\ , \quad \forall\ s \in \mathcal{S},\ t_\tau \in \mathcal{T},\ q \in \mathcal{Q}, \tag{12}$$

where f_p is a non-decreasing function with respect to (w.r.t.) the absolute value of its arguments. This ensures that the more the E-UAV user's actual departure/arrival time deviates from its preferred departure/arrival time, the higher the penalty is. Now we are ready to present the transportation agency's problem.

[3] It might appear that the problem size may become intractable if there is an unlimited number of charging levels. However, as we consider a finite number of discrete time periods, some charging levels can actually be rounded up to the same charging duration in the discrete time horizon. Therefore, there are essentially a finite number of charging level choices, namely $\mathcal{Y}$, that should be determined by the transportation agency. If the agency does not allow users to choose different charging levels, it could set $\mathcal{Y} = \emptyset$.

[4] The slight overestimation of charging time could likely enhance reliable operations of the coupled systems. For example, the extra electricity generated can serve as safety buffers for the power grid while the extra energy stored in E-UAV batteries can be used in the next trip.

2.2.2. E-UAV assignment problem

Let $x_q^{\tau,s}$ be the number of type-$q \in \mathscr{Q}$ E-UAVs that are assigned with actual departure time $t_\tau \in \mathscr{T}$ and charging station $s \in \mathscr{S}$, and let $\mathbf{x}$ be the vector collecting $x_q^{\tau,s}$,$\forall\, \tau \in \Gamma, s \in \mathscr{S}, q \in \mathscr{Q}$. Given (8)–(12), the aviation agency's E-UAV assignment problem is formulated as the following integer program (**IP1**):

$$\textbf{IP1} \quad \min_{\mathbf{x}} \sum_{\tau=1}^{T} \sum_{q\in\mathscr{Q}} \sum_{s\in\mathscr{S}} c_q(t_\tau,s)\cdot x_q^{\tau,s} \tag{13}$$

$$\text{s. t.} \sum_{\tau=1}^{T} \sum_{q\in\mathscr{Q}} x_q^{\tau,s}\cdot\zeta_q^{\tau,\tilde{\tau},s} \leqslant K_s\,, \quad \forall\, \tilde{\tau} \in \Gamma,\, s \in \mathscr{S}, \tag{14}$$

$$\sum_{\tau=1}^{T} \sum_{s\in\mathscr{S}} x_q^{\tau,s} = u_q\,, \quad \forall\, q \in \mathscr{Q}, \tag{15}$$

$$x_q^{\tau,s} \in \mathscr{N}\,, \quad \forall\, t_\tau \in \mathscr{T},\, s \in \mathscr{S},\, q \in \mathscr{Q}. \tag{16}$$

The objective (13) captures the total cost of all E-UAV users. Constraints (14) represent the capacity limit at charging stations, where K_s is the number of available charging slots at station s, and $\zeta_q^{\tau,\tilde{\tau},s}$ is a binary parameter taking value 1 if the E-UAVs of type q that start the trip at time t_τ via s will still be at this charging station until $t_{\tilde{\tau}}$; i.e., $\zeta_q^{\tau,\tilde{\tau},s} = 1$ if $t_{\tau''} \geqslant t_{\tilde{\tau}}$, and taking value 0 otherwise. Constraints (15) enforce the total demand to be satisfied, and constraints (16) define the variables to be non-negative integers. Note that this problem is essentially a minimum cost flow problem in a time-space network whose coefficients in the constraints form a totally unimodular matrix (Ahuja et al., 2014). Hence, if the demand u_q and the charging station capacity K_s are integers, solving the linear relaxation of **IP1** would still yield the optimal integer solution. Therefore, we can replace the integer value constraints (16) with the non-negativity constraints:

$$x_q^{\tau,s} \geqslant 0\,, \quad \forall\, t_\tau \in \mathscr{T},\, s \in \mathscr{S},\, q \in \mathscr{Q}. \tag{17}$$

The above formulation **IP1** will clearly yield a system-optimum solution. Moreover, Theorem 1 below implies that this solution is also an equilibrium solution for the E-UAV users.[5] The coincidence between the system optimal assignment and user equilibrium is due to the flow-independent cost functions; i.e., once the departure time and charging station is determined for a user, the assignment for other users does not affect this user's cost. To further illustrate, we let ξ_q and $v_{\tilde{\tau},s}$ denote the Lagrangian multipliers associated with total demand and charging station capacity constraints, respectively. Then we define $\tilde{c}_q(t_\tau,s) = c_q(t_\tau,s) + \sum_{\tilde{\tau}=1}^{T} \zeta_q^{\tau,\tilde{\tau},s} v_{\tilde{\tau},s}$ as the generalized travel cost of user q that is assigned with departure time t_τ and charging station s, where the first part represents the actual travel cost, and the second refers to a shadow cost for using a saturated charging station (Larsson and Patriksson, 1995; Nie et al., 2004).

Theorem 1. *Suppose* $\mathbf{x}^*$ *is an optimal solution to* **IP1***, and the agency assigns travel plans to E-UAV users based on* $\mathbf{x}^*$*. If all other users follow the agency's instructions, there is not a single user that can unilaterally reduce its generalized travel cost by not following the assigned travel plan.*

Proof. The KKT conditions for **IP1** can be written as follows:

$$x_q^{\tau,s}\left(c_q(t_\tau,s) + \sum_{\tilde{\tau}=1}^{T} \zeta_q^{\tau,\tilde{\tau},s} v_{\tilde{\tau},s} - \xi_q\right) = 0\,, \quad \forall\, q \in \mathscr{Q},\, \tau \in \Gamma,\, s \in \mathscr{S}, \tag{18}$$

$$v_{\tilde{\tau},s}\left(K_s - \sum_{\tau=1}^{T} \sum_{q\in\mathscr{Q}} x_q^{\tau,s}\zeta_q^{\tau,\tilde{\tau},s}\right) = 0\,, \quad \forall\, \tilde{\tau} \in \Gamma,\, s \in \mathscr{S}, \tag{19}$$

$$c_q(t_\tau,s) + \sum_{\tilde{\tau}=1}^{T} \zeta_q^{\tau,\tilde{\tau},s} v_{\tilde{\tau},s} - \xi_q \geqslant 0\,, \quad \forall\, q \in \mathscr{Q},\, \tau \in \Gamma, s \in \mathscr{S}, \tag{20}$$

$$v_{\tilde{\tau},s} \geqslant 0\,, \quad \forall\, \tilde{\tau} \in \Gamma,\, s \in \mathscr{S}, \tag{21}$$

and (14), (15), (17).

We can re-write (18) and (20) as

$$x_q^{\tau,s}(\tilde{c}_q(t_\tau,s) - \xi_q) = 0\,, \quad \forall\, q \in \mathscr{Q},\, \tau \in \Gamma,\, s \in \mathscr{S}, \tag{22}$$

$$\tilde{c}_q(t_\tau,s) - \xi_q \geqslant 0\,, \quad \forall\, q \in \mathscr{Q},\, \tau \in \Gamma,\, s \in \mathscr{S}. \tag{23}$$

[5] In fact, traffic assignment problems with hard capacity constraints on links usually have multiple equilibrium solutions (Nie et al., 2004). Without centralized control, one can hardly foresee in which equilibrium state the system will end up being. However, this is not the case in our model, as the aviation agency determines the assignment.

Constraints (22) and (23) state that, if all other users follow their assigned travel plan, a travel plan of an arbitrary user is used only if the generalized travel cost reaches its minimum, i.e., $x_q^{\tau,s} > 0$ only if $\tilde{c}_q(t_\tau,s) - \xi_q = 0$, and the non-used travel plans have equal or higher generalized travel cost, which completes the proof.

This theorem is quite important in our problem. As a result, the E-UAV users will have the incentive to follow the system optimum assignment from the aviation agency automatically out of their self-interest.

We have so far modeled the E-UAV user assignment problem under dynamic travel demand with limited slots at charging stations. Nonetheless, it is still unclear how the charging load at charging stations is related to the E-UAV assignment. In fact, if we denote the charging load at charging station $s \in \mathscr{S}$ at time $t_\tau \in \mathscr{T}$ by $D_{s,\tau}$, we can separate the charging cost of the E-UAV users from the transportation and unpunctuality cost, and rewrite **IP1** as:

$$\textbf{IP2} \quad \min_{\mathbf{x},\mathbf{D}} \sum_{\tau=1}^{T} \sum_{q\in\mathscr{Q}} \sum_{s\in\mathscr{S}} (c_{q,t}(t_\tau,s) + c_{q,p}(t_\tau,s))\cdot x_q^{\tau,s} + \sum_{\tau=1}^{T} \sum_{s\in\mathscr{S}} D_{s,\tau}\cdot\Delta\cdot p_{s,\tau} \tag{24}$$

$$\text{s. t.} \quad D_{s,\tau} = \sum_{\tilde{\tau}=1}^{T} \sum_{q\in\mathscr{Q}} \beta_s \zeta_q^{\tilde{\tau},\tau,s} x_q^{\tilde{\tau},s}, \quad \forall\, s \in \mathscr{S},\, \tau \in \Gamma, \tag{25}$$

$$\text{and (14),(15),(17),}$$

where Eqs. (25) map users' assigned travel plans to the electricity load at a charging station in a certain time slot. By posting varying charging prices $p_{s,\tau}$, the power system operator can influence the aviation agency's charging assignment, which in turn affects the charging load that needs to be served by the power grid.

2.3. Interactive systems operation

Now we investigate the joint operations of the coupled power and aviation transportation systems. A system-wide cost minimization problem is formulated to account for the coupling between these two systems. We show that through a joint pricing scheme of the ISO, the system optimum can be achieved for the coupled systems. For comparison, we also present a myopic pricing scheme that is widely used in practice.

2.3.1. System-wide cost minimization and joint pricing

The ISO's objective is to determine the electricity prices such that all participants' costs are minimized while the power generation meets the demand without violating the security constraints of the power system (US Federal Energy Regulatory Commission, 2003). In particular, a joint pricing scheme is needed to induce the two systems to achieve the objective.

The E-UAV charging demand $D_{s,\tau}$ for $s \in \mathscr{S}$ is computed via (25), and we let $D_{i,\tau} = 0$ for any $i \in \mathscr{B}\backslash\mathscr{S}$. Since we focus on the impact of E-UAV charging load on the grid, other types of aggregated load are treated as time-varying but fixed demand units, denoted by $U_{i,\tau}$. We use $\mathbf{D}_i \in \mathbb{R}^T$ and $\mathbf{D}_\tau \in \mathbb{R}^{|\mathscr{B}|}$ to represent the vectors of $D_{i,\tau}$ for bus $i \in \mathscr{B}\backslash\mathscr{S}$ and time slot $\tau \in \Gamma$, respectively, where $|\mathscr{B}|$ denotes the number of buses in $\mathscr{B}$. The same convention holds for the vectors $\mathbf{U}_i \in \mathbb{R}^T$ and $\mathbf{U}_\tau \in \mathbb{R}^{|\mathscr{B}|}$. By combining **IP2** and **GP**, we are now ready to present the system-wide cost minimization problem as follows:

$$\textbf{SP} \quad \min_{\mathbf{x},\mathbf{G},\mathbf{D}} Z(\mathbf{x},\mathbf{G},\mathbf{D}) := \sum_{\tau=1}^{T} \sum_{q\in\mathscr{Q}} \sum_{s\in\mathscr{S}} (c_{q,t}(t_\tau,s) + c_{q,p}(t_\tau,s))\cdot x_q^{\tau,s} + \sum_{i\in\mathscr{B}} C_i(\mathbf{G}_i) \tag{26}$$

$$s.\,t. \quad \mathbf{1}^T(\mathbf{D}_\tau + \mathbf{U}_\tau - \mathbf{G}_\tau) = 0, \quad \forall\, \tau \in \Gamma, \tag{27}$$

$$\mathbf{H}(\mathbf{D}_\tau + \mathbf{U}_\tau - \mathbf{G}_\tau) \leqslant \mathbf{C}, \quad \forall\, \tau \in \Gamma, \tag{28}$$

$$\mathbf{D}_i = \mathbf{0}, \forall\, i \in \mathscr{B}\backslash\mathscr{S}, \tag{29}$$

$$\text{(6)-(7),(14),(15),(17), and(25),}$$

where $\mathbf{D} := \{\mathbf{D}_1,\cdots,\mathbf{D}_T\}$ is a vector collection of $\mathbf{D}_\tau$, and the same convention holds for $\mathbf{G}$. The objective (26) refers to the overall system-wide cost, including the *transportation and unpunctuality cost* of the E-UAV users and the *generation cost* of the power generators. The revenue of the generators as in **GP** cancels out with the payment from the E-UAV users and the base load customers in the market (Zhang et al., 2017b). Eqs. (27) characterize the power demand/supply balance in the grid. The transmission line flow constraints under DC approximation are translated to (28), where $\mathbf{H}$ is the power transfer distribution matrix (Stott et al., 2009), and $\mathbf{C}$ is a vector of line flow limits. Meanwhile, Eqs. (6) and (7), (14), (15) and (17) are the physical constraints from the power and transportation systems, respectively.

Based on the system-wide cost minimization problem **SP**, the ISO determines the LMP. In fact, the LMP that reflects the marginal cost of power generation can be captured by the optimal Lagrangian multipliers at each bus and each time slot. The partial Lagrangian of the problem **SP** concerning only the inter-bus coupling constraints can be written as

$$\mathscr{L}_p(\mathbf{x},\mathbf{G},\mathbf{D},\boldsymbol{\gamma},\boldsymbol{\mu}) := Z(\mathbf{x},\mathbf{G},\mathbf{D}) + \sum_{\tau=1}^{T} \gamma_\tau\cdot\mathbf{1}^T(\mathbf{D}_\tau + \mathbf{U}_\tau - \mathbf{G}_\tau) + \boldsymbol{\mu}_\tau^T(\mathbf{H}(\mathbf{D}_\tau + \mathbf{U}_\tau - \mathbf{G}_\tau) - \mathbf{C}), \tag{30}$$

where $\boldsymbol{\gamma} := \gamma_\tau \in \mathbb{R}^T$ is the vector of multipliers associated with the power balance constraints (27), and $\boldsymbol{\mu}_\tau \in \mathbb{R}^{|\mathscr{I}|}$ is the multiplier of the line flow limit (28) per slot τ. As a consequence, the LMPs at various buses at time slot τ can be determined by the KKT stationarity conditions using the optimal dual variable γ_τ^* and $\boldsymbol{\mu}_\tau^*$,

$$\mathbf{p}_\tau = (\gamma_\tau^* \mathbf{1} + \mathbf{H}^T \boldsymbol{\mu}_\tau^*)/\Delta, \tag{31}$$

where the terms $\gamma_\tau^* \mathbf{1}/\Delta$ and $\mathbf{H}^T \boldsymbol{\mu}_\tau^*/\Delta$ represent the lowest cost that would be incurred for serving a load increment due to generation cost and transmission line congestion, respectively. The ISO is thus able to minimize the system-wide cost of both the aviation transportation system and the power networks by posting the optimal LMPs following (31). The following theorem characterizes the property of the solution given the optimal LMPs.

Theorem 2. *The solution to* **SP** *always exists if the feasible set described by (6) and (7), (14), (15), (17), (25) and (27)–(29) is non-empty. In addition, the solution to* **SP** *is equivalent to the solution to* **IP2** *and* **GP** *given the optimal LMPs as in (31).*

Proof. It is easy to verify that the objective of **SP** is convex w.r.t. the variables **x**,**G**, and **D**, while the constraints characterize a convex feasible set. Hence the solution to **SP** always exists, if the feasible set is non-empty (Bertsekas, 1999). In addition, based on the strong duality theory, the optimal primal variables of the **SP** would minimize the Lagrangian function at the optimal dual variable γ_τ^* and $\boldsymbol{\mu}_\tau^*$, i.e.,

$$(\mathbf{x}^*,\mathbf{G}^*,\mathbf{D}^*) = \arg \min_{\substack{\mathbf{x},\mathbf{D} \in \mathscr{F}_{\mathbf{x},\mathbf{D}} \\ \mathbf{G} \in \mathscr{F}_{\mathbf{G}}}} \mathscr{L}_p(\mathbf{x},\mathbf{G},\mathbf{D},\boldsymbol{\gamma}^*,\boldsymbol{\mu}^*), \tag{32}$$

where $\mathscr{F}_{\mathbf{G}}$ is the individual feasible set for **G** described by constraints (6) and (7), $\mathscr{F}_{\mathbf{x},\mathbf{D}}$ denotes the individual feasible set for **x**, **D** described by constraints (14), (15), (17) and (25), and $(\mathbf{x}^*,\mathbf{G}^*,\mathbf{D}^*)$ denotes the optimal solution to the **SP**. Furthermore, Eq. (32) is equivalent to

$$\begin{aligned}(\mathbf{x}^*,\mathbf{G}^*,\mathbf{D}^*) = \arg \min_{\substack{\mathbf{x},\mathbf{D} \in \mathscr{F}_{\mathbf{x},\mathbf{D}} \\ \mathbf{G} \in \mathscr{F}_{\mathbf{G}}}} & \sum_{\tau=1}^{T} \sum_{q \in \mathscr{Q}} \sum_{s \in \mathscr{S}} (c_{q,t}(t_\tau,s) + c_{q,p}(t_\tau,s)) \cdot x_q^{\tau,s} + \sum_{\tau=1}^{T} \gamma_\tau^* \cdot \mathbf{1}^T \mathbf{D}_\tau + (\boldsymbol{\mu}_\tau^*)^T \mathbf{H} \mathbf{D}_\tau + \sum_{i \in \mathscr{B}} C_i(\mathbf{G}_i) - \sum_{\tau=1}^{T} \gamma_\tau^* \cdot \mathbf{1}^T \mathbf{G}_\tau \\ -(\boldsymbol{\mu}_\tau^*)^T \mathbf{H} \mathbf{G}_\tau = & \underbrace{\operatorname{argmin}_{\mathbf{x},\mathbf{D} \in \mathscr{F}_{\mathbf{x},\mathbf{D}}} \sum_{\tau=1}^{T} \sum_{q \in \mathscr{Q}} \sum_{s \in \mathscr{S}} (c_{q,t}(t_\tau,s) + c_{q,p}(t_\tau,s)) \cdot x_q^{\tau,s} + \Delta \cdot \sum_{\tau=1}^{T} \mathbf{p}_\tau^T \mathbf{D}_\tau}_{\mathbf{IP2}} \\ + & \underbrace{\operatorname{argmin}_{\mathbf{G} \in \mathscr{F}_{\mathbf{G}}} \sum_{i \in \mathscr{B}} C_i(\mathbf{G}_i) - \Delta \cdot \sum_{\tau=1}^{T} \mathbf{p}_\tau^T \mathbf{G}_\tau}_{\mathbf{GP}}.\end{aligned} \tag{33}$$

Given the optimal LMPs **p** in (31), solving **SP** is equivalent to solving **IP2** and **GP** individually, which completes our proof.

Note that the feasibility of **SP** is required for Theorem 2 to hold. This can be readily ensured both in the model and in practice. In the model, infeasibility of **IP1** (e.g., due to insufficient total power generation capacity) can be avoided by adding a virtual charging station, which has an infinite capacity and a very high charging cost; in so doing, the solution set is always non-empty. In practice, the ISO will solve a unit commitment problem (Carrión and Arroyo, 2006) before solving the **SP** for the LMP. The solution to the unit commitment problem determines how many and which generators should be connected to the main power grid to make sure the total generation capacity is large enough to cover the presumed demand. Therefore, for simplicity, we assume that the feasibility constraints are always satisfied in our analysis.

To design the optimal LMPs, full information about the coupled systems regarding **SP** is required to be known by the ISO. However, this requirement may be impractical since the ISO can hardly access the E-UAV travel information. Motivated by the decomposable structure shown in (33), we propose a joint pricing algorithm that does not necessarily require detailed information of the E-UAV assignment. Details of the proposed algorithm are described in Section 3.

2.3.2. Myopic pricing

Before delving into our proposed pricing scheme, we introduce a naive pricing scheme for comparison purposes. This naive pricing, also referred to as *myopic pricing*, is based on the practical situation of the power and transportation systems operation nowadays, i.e., the ISO's decision-making process does not account for the coupling between the two systems. In particular, the ISO treats the charging load **D** as price-independent, and tries to minimize the total electricity generation cost under system security constraints, as follows:

$$\begin{aligned}\mathbf{MP} \quad & \min_{\mathbf{G}} \sum_{i \in \mathscr{B}} C_i(\mathbf{G}_i) \\ & s.\,t.\ (6)\text{-}(7) \text{ and } (27)\text{-}(29).\end{aligned} \tag{34}$$

At the first glance, the formulation might imply that the ISO determines the amount of electricity generation at the generators. However, it only determines the LMPs such that the overall generation cost minimization can be achieved by the self-interested generators. Similar to (31), the LMPs in the myopic pricing scheme are determined by the optimal dual variables $\hat{\gamma}_\tau$ and $\hat{\mu}_\tau$ to **MP**.

In turn, given the LMPs, the transportation agency achieves the optimal assignment as characterized by the solution to **IP2**, which

leads to a charging load **D** that will affect the solution to **MP**. Since the ISO is not aware of the flexibility of the load from the transportation system, on the next day it simply solves the **MP** based on the load data of the previous day. By iteratively solving **IP2** and **MP**, the power and transportation systems are able to interact with each other via only electricity price signals. Unfortunately, through such interactions the charging price and the load usually oscillate indefinitely, because the myopic pricing fails to account for the potential response of the transportation agency to the electricity prices; e.g., see discussions in Alizadeh et al. (2015). Through the numerical cases in Section 4, we observe such oscillations under the dynamic setting as well.

3. Solution algorithm

In this section, we develop a solution algorithm that is able to solve the problem **SP** while preserving the privacy of both the power and aviation operators. As stated in Theorem 2, an optimal solution to **SP** always exists as long as the feasible solution set is not empty. To obtain such a solution without disclosing the private information of the two infrastructures, the *dual-decomposition algorithm* can be leveraged to solve **SP** in a distributed way (Bertsekas, 1999). In particular, with the LMPs posted, **IP2** and **GP** are first solved by the aviation agency and the generators, respectively, such that the charging load **D** and power generation **G** can be determined. Then, the ISO adjusts LMPs iteratively to make the demand **D** and the generation **G** satisfy the coupling constraints (27) and (28).

To address the potential convergence issue in standard dual-decomposition algorithm with constant stepsizes, we modify the choice of stepsize so that it diminishes to zero over the iterations, but the cumulative step size is unbounded, i.e., $\theta^{(k)} \to 0$, and $\sum_k \theta^{(k)} \to \infty$ (Boyd et al., 2003). We adopt a stepsize of the following form which satisfies these conditions:

$$\theta^{(k)} = \frac{\lambda_1}{1 + \lambda_2 \cdot k^{\chi}}, \tag{35}$$

where the superscript (k) denotes the iteration index, and $\lambda_1, \lambda_2 > 0$, and power index $\chi \in (0,1)$ are constants that control the initial value and the diminishing speed of the stepsize. The proposed pricing procedure is summarized in Algorithm 1 as below:

Algorithm 1.

Step 0 Set $k = 0, \mathbf{p}^{(k)} = \mathbf{1}, \gamma^{(k)} = \mathbf{1}, \mu^{(k)} = \mathbf{0}, \theta^{(k)} = \frac{\lambda_1}{1+\lambda_2}$;
Step 1 ***Aviation Agency:*** Solve **IP1** to obtain solution $(\mathbf{x}^{(k)}, \mathbf{D}^{(k)})$,
Step 2 ***Generators:*** Solve **GP** to obtain $\mathbf{G}^{(k)}$;
Step 3 ***ISO:*** Update the stepsize $\theta^{(k+1)}$ following (35) and update the dual variables as

$$\gamma_\tau^{(k+1)} = \gamma_\tau^{(k)} + \theta^{(k+1)} \cdot \mathbf{1}^T (\mathbf{D}_\tau^{(k)} + \mathbf{U}_\tau - \mathbf{G}_\tau^{(k)}), \quad \forall \tau \in \Gamma,$$
$$\boldsymbol{\mu}_\tau^{(k+1)} = [\boldsymbol{\mu}_\tau^{(k)} + \theta^{(k+1)} \cdot (\mathbf{H}(\mathbf{D}_\tau^{(k)} + \mathbf{U}_\tau - \mathbf{G}_\tau^{(k)}) - \mathbf{C})]^+, \quad \forall \tau \in \Gamma,$$
$$\mathbf{p}_\tau^{(k+1)} = (\gamma_\tau^{(k+1)} \mathbf{1} + \mathbf{H}^T \boldsymbol{\mu}_\tau^{(k+1)})/\Delta, \quad \forall \tau \in \Gamma;$$

Let $k \leftarrow k + 1$;
Step 4 Terminate the algorithm when one of the following conditions is satisfied:
- Maximum iteration number is reached;
- The change in the LMPs $\|\mathbf{p}^{(k)} - \mathbf{p}^{(k-1)}\|$ is below ϵ.

where ϵ is a threshold value for algorithm termination. Along the iterations, **IP2** is a linear program, and **GP** is a quadratic program. They are solved by existing linear and convex optimization solvers (e.g., CPLEX/Gurobi), respectively.

The SP is solved in an iterative bidding/auction process on the day before the actual operations, following the steps in Algorithm 1. The system-wide cost minimization does not require any explicit cooperation among the ISO, the generators, and the aviation agency. To be specific, given the LMPs posted by the ISO, the generators and the aviation agency solve their own optimization problems independently, and post their generation/load bids to the ISO (Steps 1 and 2); then the ISO updates and posts the LMPs accordingly to penalize any violation of the coupling constraints (Step 3); this process is then repeated until the bids and the LMPs converge. As in Steps 1 and 2, the aviation agency and the power generators only perform their best-response to the posted LMPs, whereas they may not even be aware of the existence of each other. This property of dual-decomposition-based approach can preserve the privacy of both sides, which constitutes one of the advantages of our joint pricing scheme.

4. Numerical experiment

In this section, we run numerical experiments to evaluate the performance of the proposed joint pricing scheme under dynamic E-UAV travel demand. We compare the system performance with that under myopic pricing. Moreover, we perform sensitivity analysis over some system parameters to test the algorithm reliability and robustness.

4.1. Illustrative case study

We consider a hypothetical case of coupled power and transportation systems. On the power side, the transmission network $\mathscr{R}$ is modeled with the line and generation cost parameters of the IEEE 14-bus test case (Pierce et al., 1973). The data of the generation

Table 1
The data of the generation cost functions from IEEE 14-bus test case (Pierce et al., 1973).

Gen. #	Bus. #	$a_{i,1}$	$a_{i,2}$
1	1	0.043	20
2	2	0.25	20
3	3	0.01	40
4	6	0.01	40
5	8	0.01	40

cost functions are summarized in Table 1. Six out of nine load buses, i.e., buses 3,4,6,8,9,10, are assumed to be equipped with charging stations.

Due to the lack of a better reference, we refer to the technical specification of Tesla supercharging stations and assume that each charging slot can provide charging power up to 120 kW, i.e., $\beta_s = 0.12$ MW for all s. The time resolution for the operation of the ISO is $\Delta = 1$ h, i.e., $T = 24$ and the electricity price is determined for every hour next day. The time-varying base load is obtained by scaling the load at each bus in the nominal case obtained from the load data (MISO (2016);), i.e., the load $U_{i,\tau}$ at each bus i at time τ is computed as follows:

$$U_{i,\tau} = U_i^0 \times (h_\tau - h_{\min})/(h_{\max} - h_{\min}) , \quad \forall\, i \in \mathscr{B},\, \tau \in \Gamma,$$

where U_i^0 denotes the base load at bus i in the IEEE test case, h_τ denotes the historical average load data at time τ during a day, and $h_{\max}$ and $h_{\min}$ denote the maximum and minimal average loads during the day, respectively. The historical data $\{h_\tau\}_{\tau\in\Gamma}$ is collected from the MISO area and is averaged over days from May 1 to August 31, 2016, to represent the typical load pattern during a summer day. Three examples of time-varying base load at various buses are shown in Fig. 1.

The transportation network consists of 6 cities, each of which has exactly one charging station. Each charging station has a limit for the maximum number of E-UAVs it can serve simultaneously. The coordinates of cities are randomly generated in a rectangular plane, and the distances are calculated based on the Euclidean metric. Daily travel demand is estimated via the gravity model (Neuburger, 1971) with hypothetical attraction/production data. Given the base line travel demand, we let the actual travel demand vary over time by following a sinusoidal function, which peaks at 6 am and 6 pm, respectively. We assume the users will only charge up to the minimum required level that allows them to finish the trip. The transportation cost conversion factor α_t is set to be 1/20 ($/mile). The unpunctuality penalty function f_p is proportional to the earliness and lateness:

$$f_p(t_\tau - t_{dep}, t_{\tau''} - t_{arr}) = \alpha_p(|t_\tau - t_{dep}| + |t_{\tau''} - t_{arr}|) , \quad \forall\, q \in \mathscr{Q},\, t_\tau \in \mathscr{T},$$

where α_p is a monetary-time conversion factor, taking the value of 0.75 ($/h). Finally, to determine the charging time of each possible route, we conservatively estimate the range of a fully charged E-UAV, namely w_v, to be 150 miles for all $v \in \mathscr{V}$, and the energy-range efficiency α_v to be 1000 (mile/MWh). The other parameters are set to be $\lambda_1 = 0.03, \lambda_2 = 1.0, \chi = 0.8$, and $\epsilon = 0.5$.

The dual-decomposition algorithm was run on an Intel Core i7-4800MQ laptop, and it converges to a solution point after around 85 s until the change in the LMPs across consecutive iterations becomes negligible. The resulting charging prices and loads are demonstrated in Fig. 2, and the generation cost, the charging cost, and the transportation and unpunctuality cost are summarized in Table 2. The convergence of the algorithm is also tested by using randomized initial starting points other than the unit price, and the solution always converges to the same point within an acceptable tolerance. Moreover, for comparison (and validation), we later assume that the ISO has access to the E-UAV users' and the generators' information, and can solve **SP** directly using commercial solvers such as Gurobi. The objective values obtained from the dual-decomposition algorithm have a gap no greater than 1% compared to their counterparts from the solver.

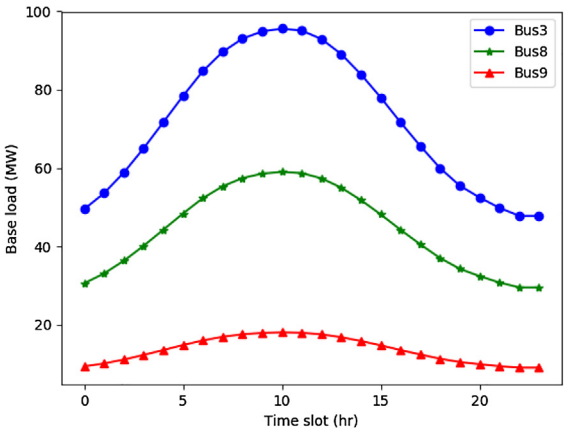

Fig. 1. Base load at three example buses, Bus 3, 8, and 9.

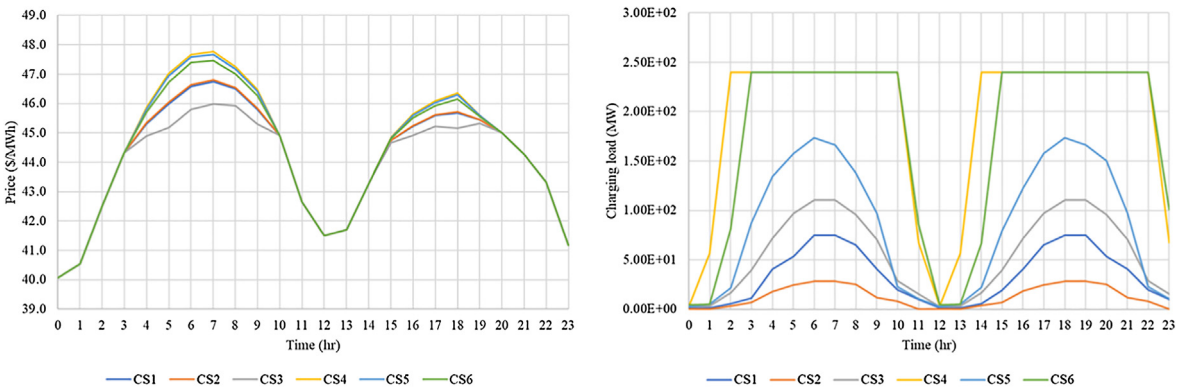

(a) Charging price (b) Charging load

Fig. 2. The convergent charging prices and loads at 6 charging stations using dynamic pricing.

Table 2
The cost resulted from the myopic pricing, static pricing, and our proposed joint and dynamic pricing method.

		Gen. cost ($)	Trans. & Unpunc. cost ($)	Charging cost ($)	System cost (Gen. + Travel) ($)
Myopic	$i = 2n$	878904.60	575417.75	592505.89	1454322.35
	$i = 2n + 1$	879520.27	569643.25	594396.15	1449163.52
Static		878729.66	547088.00	579312.79	1425817.66
Joint & Dynamic	$i = 2n$	878096.57	547130.14	600525.90	1425226.71
	$i = 2n + 1$	878096.57	547128.96	600494.19	1425225.52

4.2. Myopic vs. joint pricing

We first investigate the system performance under the *myopic pricing*. We initialize the charging price at each time and each charging station to be identical at $50/MWh, and solve the problems **MP** and **IP2** iteratively. Interestingly, as observed under the static setting in Alizadeh et al. (2015), the oscillation of the coupled system is also observed under our dynamic setting. The resulting charging price oscillates between two patterns over iterations, as illustrated in Fig. 3. As shown in Fig. 3(a), the charging prices across all charging stations peak at 7:00 and 10:00 in the even iterations $i = 2n$, which suppresses the charging demand at these time slots for the next iteration, $i = 2n + 1$. Consequently, the charging demand is re-assigned and concentrates at 5:00 and 8:00. This re-assignment of demand causes an extremely high peak of prices at 8:00 and another peak of prices at 5:00 as shown in Fig. 3(b). This induces the peak demand to other time slots and results in the price profile as in Fig. 3(a). This oscillatory phenomenon, caused by ISO's negligence of response of aviation agency to electricity prices, is detrimental to the stability of the coupled system as it induces extremely high prices at peak hours. Moreover, as the E-UAV travel demand increases, this myopic pricing method may even give rise to an *infeasible* charging load demand that cannot be satisfied by the capacity of the power network, which makes the unstable system

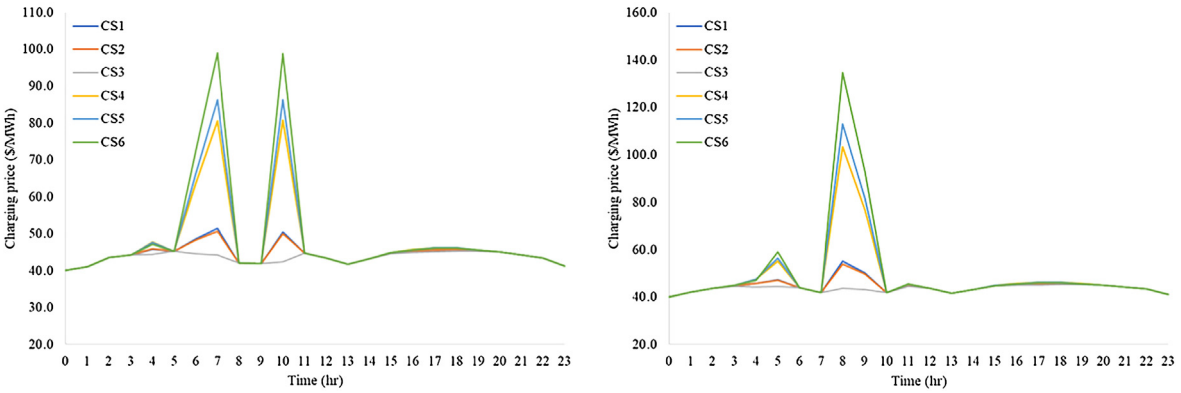

(a) Iteration $i = 2n$ (b) Iteration $i = 2n + 1$

Fig. 3. The oscillation pattern of charging prices at 6 charging stations determined by myopic pricing.

Table 3
The power imbalance across time when the static pricing result is applied onto the dynamic setting.

Time slot (h)	1	2	3	4	5	6	7	8
Power unbalance (MW)	−607.41	−528.01	−194.15	91.97	248.47	367.06	426.50	474.46
Time slot (h)	9	10	11	12	13	14	15	16
Power unbalance (MW)	421.39	333.14	194.03	−193.36	−371.96	−335.45	−57.48	162.51
Time slot (h)	17	18	19	20	21	22	23	24
Power unbalance (MW)	248.70	297.66	292.12	275.54	215.55	88.91	−64.91	−449.57

even more fragile.

In contrast, the dual-decomposition based method for our joint pricing strategy is guaranteed to converge. The convergent charging price and load profiles are illustrated in Fig. 2. It is also clear that the charging prices remain much more stable over time than either of the patterns from myopic pricing. In addition, in accordance with Table 2, our joint pricing method outperforms the myopic pricing in terms of the power generation cost, the E-UAV transportation and unpunctuality cost, and the total system-wide cost.

4.3. Static vs. dynamic pricing

Another interesting comparison is between the static/one-shot pricing and our proposed pricing that accounts for the time-varying feature of both the power and transportation systems. We take an average over the travel time and base load across the day to obtain input data to the static/time-invariant test case. In this case, the proposed dual-decomposition based pricing, i.e., Algorithm 1, can still be applied and it converges to a price profile which is constant over time.

We then post this constant price profile to the transportation agency and obtain the charging load profile under the dynamic settings. The static pricing result leads to a charging load profile that has more abrupt changes than that under our proposed pricing; this is shown in Fig. 2(b). Moreover, if the power generators produce power in response to this price by solving the **GP**, there will be an imbalance between the power generation and the demand for most of the time slots, i.e., $\mathbf{1}^T(\mathbf{D}_\tau + \mathbf{U}_\tau - \mathbf{G}_\tau) \neq 0$ for some $\tau \in \Gamma$, which, as shown in Table 3, severely challenges the security of power systems. Although there will still be some power imbalance in the joint and dynamic pricing (due to numerical convergence tolerances), such an imbalance is negligible when compared to the result of one-shot pricing. The maximum power imbalance over all periods is no greater than 0.6 MW under the joint and dynamic pricing.

4.4. Sensitivity analysis

We also perform a series of sensitivity analyses over the input data and several system parameters to test the robustness and reliability of the result. We first scale the demand up/down to examine the changes in the cost and load profile at different charging stations. Then we modify the cost parameters including α_t and α_p. These results are summarized in Table 4.

Table 4 shows that the generation cost, the transportation and unpunctuality cost, and the charging cost all change approximately proportionally to the demand, and the transportation and unpunctuality cost is more sensitive to the total demand than the generation cost. This is mainly because the limited capacity at charging stations forces some E-UAV users to be assigned to less desirable departure times, which further increases the unpunctuality penalty. Moreover, when the E-UAV travel demand increases/reduces by 10%, the total charging loads across all charging stations change by the same proportion, but the loads at each charging station increase/reduce differently. For one of the six charging stations, its total charging load over the 24-h period only has a relatively small change (e.g., about −3.7% when the demand reduces by 10%, and 8.2% when the demand increases by 10%). However, for other

Table 4
The percent changes in the cost with changed demand and cost parameters α_t and α_p, compared with the benchmark case.

		Gen. cost (%)	Trans. & Unpunc. cost (%)	Charging cost (%)	System cost (Gen. + Travel) (%)
Travel demand u_q	+10%	+6.6	+12.4	+10.6	+8.8
	+5%	+3.3	+6.2	+5.3	+4.4
	−5%	−3.3	−5.9	−5.3	−4.3
	−10%	−6.7	−11.6	−10.7	−8.5
Transportation cost coefficient α_t	+10%	±0.0	+9.8	+0.1	+3.8
	+5%	±0.0	+4.9	+0.1	+1.9
	−5%	±0.0	−4.9	±0.0	−1.9
	−10%	±0.0	−9.8	±0.0	−3.8
Unpunctuality penalty coefficient α_p	+10%	±0.0	+0.2	±0.0	+0.1
	+5%	±0.0	+0.1	±0.0	±0.0
	−5%	±0.0	−0.1	+0.1	±0.0
	−10%	±0.0	−0.2	+0.1	−0.1

charging stations the total load change can be as significant as −16.5% when the demand decreases, corresponding to an 334.8 MWh drop in energy consumption, or 10.3% when the demand is increased, corresponding to a 207.4 MWh increment in energy consumption. Meanwhile, the results suggest that the LMPs at the charging stations are indeed sensitive to the changes in the demand.

The results in Table 4 also suggest that the total system-wide cost is not very sensitive to the cost coefficients α_t and α_p. This is good. When α_t increases/decreases by 10%, the transportation and unpunctuality cost changes by approximately + 9.8% and −9.8%, respectively; the transportation and unpunctuality cost is even less sensitive to α_p, as the percent changes are only + 0.2% and −0.2% when α_p is increased/reduced by 10%, respectively. The E-UAVs assignment does not appear to be very sensitive to the changes in travel cost coefficients. This is probably due to the limited number of charging station choices in this specific case. It implies that the usage of charging stations is not noticeably changed when there is a small perturbation to the system coefficients. There is not any significant change in the LMPs either when we perturb α_t or α_p, as the LMPs are determined by the travel demand and the power generation at the buses, which are both insensitive to the change in the cost coefficients.

5. Conclusion

With the rapid development of E-UAV technologies, we envision that E-UAVs will be widely used for freight or passenger shipments in the near future, and E-UAVs' en-route charging needs at the commercial scale may impose non-negligible impacts on the power systems' operations. In this paper, we investigate the joint operations of coupled power and electric aviation transportation systems, where the travel demand and the power system base load vary over time. The power-side ISO determines and posts electricity prices to the generators and users, while an aviation transportation agency centrally controls the E-UAV users by optimally assigning charging location and schedules. We formulate a system-wide total cost minimization problem for the coupled systems, where a dynamic E-UAV charging assignment model is embedded to smooth the power system loads. A joint pricing scheme is developed to achieve system-wide optimum for the coupled systems. Numerical experiments are conducted to demonstrate that the proposed joint dynamic pricing scheme outperforms the myopic as well as static pricing strategies in terms of producing more stable electricity prices and more balanced load profile, which essentially improves the overall performance of the coupled systems operation.

We understand that there are enormous uncertainties associated with future E-UAV technological breakthroughs, especially those regarding battery and charging efficiency. As a result, it is difficult to envision the exact pathway of the E-UAV industry in the future. Battery ranges and charging time, for example, may affect people's perception on distances and choices over transportation modes, which in turn determine the viability of the entire industry. However, given the rapid advances of E-UAV technologies, we believe that the future of the industry is promising, and it is meaningful to discuss possible scenarios and the associated challenges. This paper acts as an initial step toward this exciting and yet ambitious goal, and we see several interesting directions for future exploration.

First, this paper mainly focuses on mid-range intercity E-UAV trips with origin-destination-based demand. Other types of demand description are certainly worth investigating, as applications of E-UAVs to both freight delivery and passenger transportation have been continuously increasing. For example, for short-distance intra-city trips, activity-based or trip-chain demand models may better capture people's travel behaviors as well as charging decisions among trips. In addition, since most charging activities for such trips happen at destinations (e.g., workplaces or households), we are also interested in investigating how to characterize the impacts of destination charging loads of E-UAVs on the power grid, while considering the possibility of rescheduling the E-UAV charging loads to low-power-consumption hours, by applying smart grid technologies (e.g., the "demand response program" (Aalami et al., 2010) for the household power supply). Moreover, as low-altitude aircraft congestions will almost certainly arise when the population of E-UAVs grows large, we are interested in investigating the operations of the aviation transportation and the power system while considering the traffic route choices under congestion in a continuous space (e.g., (Ouyang et al., 2015; Wang and Ouyang, 2018; Wang et al., 2018)).

Second, it would also be interesting to investigate how the proposed modeling framework can be extended to accommodate other E-UAV business scenarios, especially when some other entities and/or participants enter the E-UAV transportation industry as well as the electricity market in the future. For instance, if E-UAVs are owned and run by a company or an agency, some operational issues such as empty E-UAV relocations (similar to the fleet management problem (Simao et al., 2009; Hajibabai and Ouyang, 2016)), the E-UAV recharging routing and scheduling (similar to the refueling routing and scheduling problem (Nourbakhsh and Ouyang, 2010; Hajibabai et al., 2014)) may rise, and certain technology-enabled operational strategies (such as battery swap, V2G charging/discharging scheduling) may possibly be worth investigating. Moreover, the charging stations may be owned and operated by a profit-seeking entity, which may not be willing to post the same LMPs as those determined by the ISO. Therefore, another interesting topic would be to incorporate gaming behavior among stakeholders into the design and analysis of a profit-seeking charging pricing scheme.

Furthermore, in the more distant future, once operational rules and regulations are ready, demand-responsive E-UAV service may become possible and trips may no longer be centrally controlled by the aviation agency. Such operations would inevitably cause congestions at the charging stations and unexpected power load fluctuations. It is hence worth investigating the impacts of stochastic travel demand and charging loads of the E-UAVs on the power grid in a real-time electricity market, in the hope of finding optimal electricity generation and pricing strategies under both day-ahead commitments and real-time random demand.

Finally, instead of focusing solely on the daily operations of the power and the transportation systems, we are also interested in their long-term planning process. For example, as the population of E-UAVs gets larger and the associated system becomes increasingly complex, it would become even more critical to have a reliable and sustainable E-UAV charging infrastructure system.

Based on the existing studies on electric vehicle charging infrastructure design problem (He et al., 2013, 2015), we can foresee that the optimal design and deployment of E-UAV charging infrastructures, while considering the daily operations of power and transportation systems would be a challenging problem.

Acknowledgment

This study is financially supported in part by the Institute for Sustainability, Energy, and Environment (iSEE) at the University of Illinois. The authors are part of an inter-disciplinary group that is working on a project titled “Interdependent Critical Infrastructure Systems for Synergized Utilization of Multiple Energy Sources Toward Sustainable Vehicular Transportation.” Partial financial support was also provided by the National Science Foundation via Grant CMMI-1662825. Very helpful comments from the three anonymous reviewers are also gratefully acknowledged.

References

Aalami, H., Moghaddam, M.P., Yousefi, G., 2010. Modeling and prioritizing demand response programs in power markets. Electr. Power Syst. Res. 80 (4), 426–435.
Adler, J.D., Mirchandani, P.B., Xue, G., Xia, M., 2016. The electric vehicle shortest-walk problem with battery exchanges. Networks Spat. Econ. 16 (1), 155–173.
Agatz, N., Bouman, P., Schmidt, M., 2018. Optimization approaches for the traveling salesman problem with drone. Transport. Sci. Art. Adv. http://dx.doi.org/10.1287/trsc.2017.0791.
Ahuja, R.K., Magnanti, T.L., Orlin, J.B., 2014. Network Flows. Pearson Education. Harlow, UK.
Alizadeh, M., Wai, H.-T., Chowdhury, M., Goldsmith, A., Scaglione, A., Javidi, T., 2015. Optimal pricing to manage electric vehicles in coupled power and transportation networks. IEEE Trans. Control Network Syst. 4 (4), 863–875.
Bertsekas, D.P., 1999. Nonlinear Programming. Athena Scientific, Belmont, MA.
Boyd, S., Xiao, L., Mutapcic, A., 2003. Subgradient Methods. Lecture notes of EE392o, Stanford University, Autumn Quarter.
Carrión, M., Arroyo, J.M., 2006. A computationally efficient mixed-integer linear formulation for the thermal unit commitment problem. IEEE Trans. Power Syst. 21 (3), 1371–1378.
Chen, Z., He, F., Yin, Y., 2016. Optimal deployment of charging lanes for electric vehicles in transportation networks. Transport. Res. Part B: Methodol. 91, 344–365.
Dorling, K., Heinrichs, J., Messier, G.G., Magierowski, S., 2017. Vehicle routing problems for drone delivery. IEEE Trans. Syst., Man, Cybernet.: Syst. 47 (1), 70–85.
Etherington, D., 2017. Zunum Aeros Electric Passenger Plane Hopes to offer Cheaper Flights by 2020. < http://social.techcrunch.com/2017/04/05/zunum-aeros-electric-passenger-plane-hopes-to-offer-cheaper-flights-by-2020 > .
Ferrandez, S.M., Harbison, T., Weber, T., Sturges, R., Rich, R., 2016. Optimization of a truck-drone in tandem delivery network using K-means and genetic algorithm. J. Ind. Eng. Manage. 9 (2), 374–388.
Glover, J.D., Sarma, M.S., Overbye, T., 2011. Power System Analysis & Design, SI Version. Cengage Learning. Stamford, Connecticut.
Guerriero, F., Surace, R., Loscr, V., Natalizio, E., 2014. A multi-objective approach for unmanned aerial vehicle routing problem with soft time windows constraints. Appl. Math. Model. 38 (3), 839–852.
Ha, Q.M., Deville, Y., Pham, Q.D., H, M.H., Sep. 2015. On the Min-cost Traveling Salesman Problem with Drone. Available from: < arXiv:1509.08764 > [cs]. < http://arxiv.org/abs/1509.08764 > .
Hajibabai, L., Nourbakhsh, S., Ouyang, Y., Peng, F., 2014. Network routing of snowplow trucks with resource replenishment and plowing priorities: formulation, algorithm, and application. Transport. Res. Rec.: J. Transport. Res. Board (2440), 16–25.
Hajibabai, L., Ouyang, Y., 2016. Dynamic snow plow fleet management under uncertain demand and service disruption. IEEE Trans. Intell. Transport. Syst. 17 (9), 2574–2582.
Ham, A.M., 2018. Integrated scheduling of m-truck, m-drone, and m-depot constrained by time-window, drop-pickup, and m-visit using constraint programming. Transport. Res. Part C: Emerg. Technol. 91, 1–14.
Hawkins, A.J., 2017. Watch this All-electric “flying car take its first test flight in Germany. < https://www.theverge.com/2017/4/20/15369850/lilium-jet-flying-car-first-flight-vtol-aviation-munich > .
He, F., Wu, D., Yin, Y., Guan, Y., 2013. Optimal deployment of public charging stations for plug-in hybrid electric vehicles. Transport. Res. Part B: Methodol. 47, 87–101.
He, F., Yin, Y., Lawphongpanich, S., 2014. Network equilibrium models with battery electric vehicles. Transport. Res. Part B: Methodol. 67, 306–319.
He, F., Yin, Y., Zhou, J., 2015. Deploying public charging stations for electric vehicles on urban road networks. Transport. Res. Part C: Emerg. Technol. 60, 227–240.
Hern, A., 2014. DHL Launches First Commercial Drone “parcelcopter” Delivery Service. < http://www.theguardian.com/technology/2014/sep/25/german-dhl-launches-first-commercial-drone-delivery-service > .
Hobbs, B.F., Metzler, C.B., Pang, J.-S., 2000. Strategic gaming analysis for electric power systems: An MPEC approach. IEEE Trans. Power Syst. 15 (2), 638–645.
Hong, I., Kuby, M., Murray, A.T., 2018. A range-restricted recharging station coverage model for drone delivery service planning. Transport. Res. Part C: Emerg. Technol. 90, 198–212.
Kaufmann, S., Kerner, B.S., Rehborn, H., Koller, M., Klenov, S.L., 2018. Aerial observations of moving synchronized flow patterns in over-saturated city traffic. Transport. Res. Part C: Emerg. Technol. 86, 393–406.
Kim, J., Morrison, J.R., 2014. On the concerted design and scheduling of multiple resources for persistent UAV operations. J. Intell. Robot. Syst. 74 (1–2), 479–498.
Kim, J., Song, B.D., Morrison, J.R., 2013. On the scheduling of systems of UAVs and fuel service stations for long-term mission fulfillment. J. Intell. Robot. Syst. 70 (1–4), 347–359.
Kim, S.J., Lim, G.J., Cho, J., Ct, M.J., 2017. Drone-aided healthcare services for patients with chronic diseases in rural areas. J. Intell. Robot. Syst. 1–18.
Larsson, T., Patriksson, M., 1995. An augmented Lagrangean dual algorithm for link capacity side constrained traffic assignment problems. Transport. Res. Part B: Methodol. 29 (6), 433–455.
Luo, Z., Liu, Z., Shi, J., 2017. A two-echelon cooperated routing problem for a ground vehicle and its carried unmanned aerial vehicle. Sensors 17 (5), 1144.
Ma, Z., Callaway, D., Hiskens, I., 2012. Optimal charging control for plug-in electric vehicles. In: Control and Optimization Methods for Electric Smart Grids. Springer, pp. 259–273.
Maini, P., Sujit, P.B., 2015. On cooperation between a fuel constrained UAV and a refueling UGV for large scale mapping applications. In: 2015 International Conference on Unmanned Aircraft Systems (ICUAS), pp. 1370–1377.
Mattise, N., 2013. Amazon unveils “Prime Air, a plan to deliver by drone in just 30 minutes. < https://arstechnica.com/gadgets/2013/12/forget-amazons-two-day-shipping-soon-you-can-select-drone-delivery > .
MISO, 2016. MISO real-time historical load data. < https://www.misoenergy.org/MarketsOperations/RealTimeMarketData/Pages/RealTimeTotalLoad.aspx > (accessed on 2017-07-31).
Muoio, D., 2016. This company says it’s ready to build a real flying car — here’s how it works. < http://www.businessinsider.com/terrafugia-could-have-flying-car-ready-in-2025-2016-8 > .
Muoio, D., 2017. Mercedes’ parent company is making a big investment in a flying taxi startup — here’s what we know. < http://www.businessinsider.com/volocopter-flying-taxi-30-million-funding-daimler-2017-8 > .
Murray, C.C., Chu, A.G., 2015. The flying sidekick traveling salesman problem: optimization of drone-assisted parcel delivery. Transport. Res. Part C: Emerg. Technol.

54, 86–109.
Neuburger, H., 1971. User benefit in the evaluation of transport and land use plans. J. Transp. Econ. Policy 52–75.
Nie, Y., Zhang, H., Lee, D.-H., 2004. Models and algorithms for the traffic assignment problem with link capacity constraints. Transport. Res. Part B: Methodol. 38 (4), 285–312.
Nintanavongsa, P., Yaemvachi, W., Pitimon, I., 2016. A self-sustaining unmanned aerial vehicle routing protocol for smart farming. In: 2016 International Symposium on Intelligent Signal Processing and Communication Systems (ISPACS), pp. 1–5.
Nourbakhsh, S.M., Ouyang, Y., 2010. Optimal fueling strategies for locomotive fleets in railroad networks. Transport. Res. Part B: Methodol. 44 (8-9), 1104–1114.
Ouyang, Y., Wang, Z., Yang, H., 2015. Facility location design under continuous traffic equilibrium. Transport. Res. Part B: Methodol. 81, 18–33.
Pierce Jr., H., Colborn, H., Coleman, D., Marriage, E., Richard, J., Rindt, L., Rubino, L., Stagg, G., Traub, T., Vandergrift, J., et al., 1973. Common format for exchange of solved load flow data. IEEE Trans. Power Apparat. Syst. 92 (6), 1916–1925.
Poikonen, S., Wang, X., Golden, B., 2017. The vehicle routing problem with drones: extended models and connections. Networks 70 (1), 34–43.
Pugliese, L.D.P., Guerriero, F., Zorbas, D., Razafindralambo, T., 2016. Modelling the mobile target covering problem using flying drones. Optim. Lett. 10 (5), 1021–1052.
Simao, H.P., Day, J., George, A.P., Gifford, T., Nienow, J., Powell, W.B., 2009. An approximate dynamic programming algorithm for large-scale fleet management: a case application. Transport. Sci. 43 (2), 178–197.
Song, B.D., Kim, J., Kim, J., Park, H., Morrison, J.R., Shim, D.H., 2014. Persistent UAV service: an improved scheduling formulation and prototypes of system components. J. Intell. Robot. Syst. 74 (1–2), 221–232.
Song, B.D., Kim, J., Morrison, J.R., 2016. Rolling horizon path planning of an autonomous system of UAVs for persistent cooperative service: MILP formulation and efficient heuristics. J. Intell. Robot. Syst. 84 (1–4), 241–258.
Stewart, J., 2014. Google tests drone deliveries in Project Wing trials. < http://www.bbc.com/news/technology-28964260 > .
Stott, B., Jardim, J., Alsaç, O., 2009. DC power flow revisited. IEEE Trans. Power Syst. 24 (3), 1290–1300.
Sundar, K., Rathinam, S., 2012. Route planning algorithms for unmanned aerial vehicles with refueling constraints. In: 2012 American Control Conference (ACC), pp. 3266–3271.
Sundar, K., Rathinam, S., 2014. Algorithms for routing an unmanned aerial vehicle in the presence of refueling depots. IEEE Trans. Autom. Sci. Eng. 11 (1), 287–294.
Sweda, T.M., Klabjan, D., 2012. Finding minimum-cost paths for electric vehicles. In: 2012 IEEE International Electric Vehicle Conference (IEVC), pp. 1–4.
Thiels, C.A., Aho, J.M., Zietlow, S.P., Jenkins, D.H., 2015. Use of unmanned aerial vehicles for mddical product transport. Air Med. J. 34 (2), 104–108.
US Federal Energy Regulatory Commission, 2003. White Paper: Wholesale Power Market Platform. Tech. Rep., Washington, D.C.
Vanian, J., 2017. UPS has a new trick to make drone deliveries a reality. < http://fortune.com/2017/02/21/ups-drone-deliveries-florida/ > .
Wang, X., Poikonen, S., Golden, B., 2017. The vehicle routing problem with drones: several worst-case results. Optim. Lett. 11 (4), 679–697.
Wang, Z., Ouyang, Y., 2018. On solving a class of continuous traffic equilibrium problems and planning facility location under congestion. Oper. Res. (revision under review).
Wang, Z., Xie, S., Ouyang, Y., 2018. Reliable facility location under continuous traffic equilibrium and disruption risks. Working Paper. University of Illinois Urbana-Champaign.
Worley, O., Klabjan, D., 2011. Optimization of battery charging and purchasing at electric vehicle battery swap stations. In: 2011 IEEE Vehicle Power and Propulsion Conference (VPPC), pp. 1–4.
Worley, O., Klabjan, D., Sweda, T.M., 2012. Simultaneous vehicle routing and charging station siting for commercial electric vehicles. In: 2012 IEEE International Electric Vehicle Conference (IEVC), pp. 1–3.
Xu, H., Zhang, K., Zhang, J., 2017. A tri-level model for optimal bidding and pricing of profit-seeking load serving entity. Available from: arXiv preprint < arXiv:1708.04645 > .
Xu, Y., Pan, F., 2012. Scheduling for charging plug-in hybrid electric vehicles. In: 2012 IEEE 51st Annual Conference on Decision and Control (CDC), pp. 2495–2501.
Zhang, K., Zhu, H., Guo, S., 2017a. Dependency analysis and improved parameter estimation for dynamic composite load modeling. IEEE Trans. Power Syst. 32 (4), 3287–3297.
Zhang, Y., Yang, R., Zhang, K., Jiang, H., Zhang, J.J., 2017b. Consumption behavior analytics-aided energy forecasting and dispatch. IEEE Intell. Syst. 32 (4), 59–63.